

Commun. Theor. Phys. **73** (2021) 125004 (11pp) https://doi.org/10.1088/1572-9494/ac2e6a

A spin-less particle on a rotating curved surface in Minkowski space

Run Cheng[1,2], Li Wang[1], Hao Zhao[1,2], Cui-Bai Luo[3], Yong-Long Wang[2] and Jun Wang[1,*]

[1] National Lab of Solid State Microstructure, Collaborative Innovation Center of Advanced Microstructures, and School of Physics, Nanjing University, Nanjing 210093, China
[2] School of Physics and Electronic Engineering, Linyi University, Linyi 276005, China
[3] Department of Physics, Anhui Normal University, Wuhu 241002, China

E-mail: wangyonglong@lyu.edu.cn and wangj@nju.edu.cn

Received 12 August 2021, revised 22 September 2021
Accepted for publication 11 October 2021
Published 12 November 2021

Abstract

In Minkowski space $\mathcal{M}$, we derive the effective Schrödinger equation describing a spin-less particle confined to a rotating curved surface $\mathcal{S}$. Using the thin-layer quantization formalism to constrain the particle on $\mathcal{S}$, we obtain the relativity-corrected geometric potential V_g', and a novel effective potential $\tilde{V}_g$ related to both the Gaussian curvature and the geodesic curvature of the rotating surface. The Coriolis effect and the centrifugal potential also appear in the equation. Subsequently, we apply the surface Schrödinger equation to a rotating cylinder, sphere and torus surfaces, in which we find that the interplays between the rotation and surface geometry can contribute to the energy spectrum based on the potentials they offer.

Keywords: rotating curved surface, Minkowski space, surface Schrödinger equation, curvature

(Some figures may appear in colour only in the online journal)

1. Introduction

Quantum physics on a curved surface has attracted much attention in recent years, accompanied with the development of low-dimensional materials [1–4]. It is observed that the curvature of a surface may produce systematic effects on the energy spectrum and dynamics of quantum systems [5–9]. These observations demonstrate the importance of spatial geometry, and stimulated the discovery of several low-dimensional structures with novel quantum behaviors.

In physics, there is another source that produces spatial curvature, that is, the relativistic effect. This was suggested historically for a rotating disc by Ehrenfest [10]. For such a disc, the circumference experiences the Lorentz contraction, while the radial elements do not contract because their motion is normal to their lengths [11]. With this kind of relativistic effect, the ratio between the circumference and the radius of a rotating disc would be smaller than 2π, which implies an effective geodesic curvature. This kind of effective curvature can also alter the quantum behaviors on the disc [12], representing another contribution of spatial geometry. Note that the curvatures from the relativistic effect and from the intrinsic geometry often occur simultaneously on a rotating surface. Since these two kinds of geometric effects are different in their relations to the quantum behaviors and cannot be described with a single curvature parameter, how to determine the quantum behaviors on a rotating surface is a non-trivial problem.

In recent decades, the quantum physics on a rotating surface attracted more practical concerns to understand the energetic spectra of low-dimensional nanostructures [13–16]. Not only may some molecules (i.e. C_{60}) rotate fast under thermal equilibrium, but also some larger nanostructures can be driven to rotate more quickly based on the evolving nano-electro-mechanical [17] and synthesis technology [18–20]. For example, the nanoscale rotational actuators based on carbon nanotubes are successfully fabricated [21], the realization of ultra-fast rotating carbon nanotubes obtained from circularly polarized light is addressed in [22, 23], and the controllable high-speed rotating nanowires can be achieved by ac voltage applied to multiple electrodes [24]. These experimental progresses demand proper theory to quantitatively characterize quantum physics related to the rotational surface. Recently, the

* Author to whom any correspondence should be addressed.

non-trivial rotation effects on the electronic structure of carbon nanomaterials, including rotating fullerene and rotating carbon nanotube, have been widely discussed [25–28]. However, there are no theories to consider both the Gaussian curvature of the surface and the geodesic curvature related to the relativity effect, which are intrinsic in the rotating nanostructures. How do these two effects interplay with each other and modulate the quantum behaviors on the rotating surface? Our work is an approach towards such a problem theoretically.

In our work, we focus on the quantum dynamics of a spin-less particle on several 2D rotating curved surfaces. The thin-layer quantization formalism [29–31] is carried out to constrain the particle on the rotating surfaces. The special relativity is incorporated to characterize the relativistic effect on the geometry [11]. To explicitly exemplify the contribution and interplay of two kinds of geometric effects, an effective Schrödinger equation for the rotating curved surfaces in Minkowski space is proposed based on the assumed wave functions. In this equation, the geometric potential still exists and is corrected by the relativistic effect, but also a novel effective potential related to both kinds of curvatures is observed. With these effective potentials, the contributions of rotational motion on the energy spectrum are discussed. These establish a procedure to analyze the quantum behaviors on the rotating surfaces.

The outline for our paper is given as follows. In section 2, the proper length measured in a rotating frame is given in terms of the special relativity. In section 3, we derive the effective Schrödinger equation for a spin-less particle confined to a rotating curved surface $\mathcal{S}$ in Minkowski space $\mathcal{M}$. In sections 4–6, based on the surface Schrödinger equation, the behavior of the particle on the rotating cylinder, sphere and torus surfaces are specifically analyzed, focusing on the curvature effects of the relativity and the intrinsic geometry. Finally, we draw our conclusions in section 7.

2. Proper length measured in rotating frame

In this section, the proper length measured in a rotating frame should be given in terms of the special relativity. The study begins with the line element in Minkowski space:

$$\mathrm{d}s^2 = g_{00}(\mathrm{d}x^0)^2 + 2g_{0i}\mathrm{d}x^0\mathrm{d}x^i + g_{ik}\mathrm{d}x^i\mathrm{d}x^k, \tag{1}$$

where $x^0 = ct$, $x^i(x^k)$ are coordinate components, $i(k) = 1, 2, 3$ and $g_{00} = -1$. For two adjacent points A and B, the proper length $\mathrm{d}l$ can be determined as $\mathrm{d}l = \sqrt{\mathrm{d}s^2}$ when the coordinate clocks of the two points are synchronous. Note that, in the rotating frame, the synchrony of two coordinate clocks does not correspond to $\mathrm{d}x^0 = 0$. The standard synchrony of two clocks located at A and B can be defined based on a light signal which follows a null-geodesics (i.e. $\mathrm{d}s = 0$). That is, a light signal is sent from A to B and is reflected back to A. Measured by the observer at A, the coordinate times to send, to receive, and to reflect the light signal are $x^0_{A\rightarrow}$, $x^0_{A\leftarrow}$, and x^0_A, respectively. Clearly, we have the relation $x^0_A = (x^0_{A\rightarrow} + x^0_{A\leftarrow})/2$. Corresponding the reflecting event, the coordinate time of the clock at B is x^0_B, which is synchronized with the coordinate time x^0_A at A. Therefore, when two remote events occur synchronously, the coordinate clocks differ by:

$$\Delta x^0 = x^0_A - x^0_B \equiv \frac{\mathrm{d}x^0_{A\rightarrow B} + \mathrm{d}x^0_{A\leftarrow B}}{2}, \tag{2}$$

where $\mathrm{d}x^0_{A\rightarrow B} \equiv x^0_{A\rightarrow} - x^0_B$ and $\mathrm{d}x^0_{A\leftarrow B} \equiv x^0_{A\leftarrow} - x^0_B$.

According to the null-geodesics relation, the propagation of the light signal obeys the relation

$$\mathrm{d}x^0 = \frac{-g_{0i}\mathrm{d}x^i \pm \sqrt{(g_{0i}g_{0k} - g_{00}g_{ik})\mathrm{d}x^i\mathrm{d}x^k}}{g_{00}}. \tag{3}$$

Therefore, $\Delta x^0 = -g_{0i}\mathrm{d}x^i/g_{00}$. Substituting this relation into equation (1), the proper length between two neighboring points is

$$\begin{aligned} \mathrm{d}l^2 &= \gamma_{ik}\mathrm{d}x^i\mathrm{d}x^k, \\ \gamma_{ik} &\equiv g_{ik} - \frac{g_{0i}g_{0k}}{g_{00}}, \end{aligned} \tag{4}$$

where γ_{ik} is a pure spatial metric, and $\mathrm{d}l$ is a pure spatial distance between A and B measured in rotating frame.

3. Effective Schrödinger equation for a spin-less particle constrained on a rotating curved surface

In this section, in the spirit of the thin-layer quantization formalism, the effective Schrödinger equation for a spin-less particle confined to a rotating curved surface in the context of special relativity is given. The effects both from the curved surface and from the relativity are considered.

The study begins with a curved surface $\mathcal{S}$ rotating around any axis $\vec{e}_\varepsilon$ at a constant angular velocity $\vec{\omega}$ embedded in the Minkowski space $\mathcal{M}$. The line element over $\mathcal{S}$ can be described as:

$$\mathrm{d}s^2 = g_{\mu\nu}\mathrm{d}x^\mu\mathrm{d}x^\nu, \quad \mu, \nu = 0, 1, 2, \tag{5}$$

where x^μ, x^ν are the time-spatial coordinates of $\mathcal{M}$. Through the coordinate transformation from the stationary coordinate system to the rotating coordinate system, using the equation (4), the two-dimensional spatial distance is written as:

$$\mathrm{d}l^2 = \gamma_{ik}\mathrm{d}q^i\mathrm{d}q^k, \tag{6}$$

where $i, k = 1, 2$, q^1 and q^2 are the curvilinear coordinates over $\mathcal{S}$. Here, the covariant components of rotating surface metric tensors γ_{ik} can be obtained from equation (4). Correspondingly, based on the curvilinear coordinates, the metric tensor Γ_{ab} of the embeded 3D space can be defined as:

$$\begin{aligned} &\Gamma_{ab} = \gamma_{ab} + [\alpha\gamma + (\alpha\gamma)^T]_{ab}q^3 + (\alpha\gamma\alpha^T)_{ab}(q^3)^2, \\ &\Gamma_{3b} = \Gamma_{a3} = 0, \quad \Gamma_{33} = 1, \end{aligned} \tag{7}$$

where $a, b = 1, 2$, q^3 is the curvilinear coordinate along normal unit basis vector $\vec{e}_n$, and α is the Weingarten curvature matrix [30].

Following [12], the Hamiltonian for a spin-less particle with effective mass m on the rotating curved surface $\mathcal{S}$ reads:

$$\begin{aligned} H &= \frac{1}{2m}\left[\frac{\hbar}{i}\nabla - m\vec{\omega}\times\vec{r}\right]^2 + V_\lambda \\ &= -\frac{\hbar^2}{2m}\nabla^2 + \mathrm{i}\frac{\hbar}{2}\nabla\cdot(\vec{\omega}\times\vec{r}) + i\frac{\hbar}{2}(\vec{\omega}\times\vec{r})\cdot\nabla \\ &\quad + \frac{1}{2}m(\vec{\omega}\times\vec{r})^2 + V_\lambda, \end{aligned} \tag{8}$$

where a squeezing potential $V_\lambda(q^3)$ is introduced [29, 30] to localize the particle on surface $\mathcal{S}$, and λ is a parameter controlling the strength of the confinement. In these terms, the second term $\nabla\cdot(\vec{\omega}\times\vec{r})$ in equation (8) is always equal to 0, because that $\vec{\omega}$ is a constant vector. At the same time, the other terms can be expressed with the metrics Γ_{ab} and γ_{ik}. According to the equation (7), the laplace operator in equation (8) can be expanded as:

$$\begin{aligned} \nabla^2 &= \frac{1}{\sqrt{\Gamma}}\partial_a(\sqrt{\Gamma}\,\Gamma^{ab}\partial_b) \\ &= \frac{1}{\sqrt{\gamma}}\partial_i(\sqrt{\gamma}\gamma^{ik}\partial_k) + \frac{1}{\sqrt{\Gamma}}\partial_3(\sqrt{\Gamma}\,\partial_3), \end{aligned} \tag{9}$$

where Γ and γ are the determinants of Γ_{ab} and γ_{ik}, respectively. The Coriolis term can be rewritten as

$$\mathrm{i}\frac{\hbar}{2}(\vec{\omega}\times\vec{r})\cdot\nabla = -\frac{1}{2}\gamma_{ab}\omega^a\hat{L}^b, \tag{10}$$

with $\hat{L}^b = -\mathrm{i}\hbar\epsilon^b_{ac}r^a\nabla^c$ being the angular momentum operator. The centrifugal potential can be expressed as:

$$\frac{m}{2}(\vec{\omega}\times\vec{r})^2 = \frac{m}{2}\gamma_{ab}V^aV^b, \tag{11}$$

in which $V^a = \epsilon^a_{bc}\omega^b r^c$. Based on these derivations, the effective Schrödinger equation for the wave function $\psi(q^1, q^2, q^3)$ can be obtained as:

$$\begin{aligned} E\psi &= -\frac{\hbar^2}{2m}\frac{1}{\sqrt{\Gamma}}\partial_a(\sqrt{\Gamma}\,\Gamma^{ab}\partial_b)\psi \\ &\quad - \frac{1}{2}\gamma_{ab}\omega^a\hat{L}^b\psi + \frac{m}{2}\gamma_{ab}V^aV^b\psi + V_\lambda\psi, \end{aligned} \tag{12}$$

where E represents the eigenenergy of the particle.

To simplify the effective Schrödinger equation, according to equation (9), and we are searching for a surface function depending only on the variables q^1 and q^2 [29, 30], we naturally introduce a new wave function $\chi(q^1, q^2, q^3)$ as

$$\chi = \Gamma^{1/4}\psi = \chi_s(q^1, q^2)\chi_n(q^3), \tag{13}$$

where χ_s, χ_n are wave functions defined on the surface and along the normal direction. The introduction of the squeezing potential V_λ makes this kind of separation is generally valid in the limit that q_3 goes to zero [29, 30]. Under such a circumstance, we decouple the Schrödinger equation into a surface part and a normal part by substituting equation (13) into equation (12), as:

$$\begin{aligned} E_s\chi_s &= -\frac{\hbar^2}{2m}\gamma^{ik}\partial_i(\partial_k\chi_s) + (\tilde{V}_g + V_g')\chi_s \\ &\quad -\frac{1}{2}\gamma_{ab}\omega^a\hat{L}^b\chi_s + \frac{m}{2}\gamma_{ab}V^aV^b\chi_s, \\ E_n\chi_n &= -\frac{\hbar^2}{2m}\frac{\partial^2\chi_n}{\partial q^{3^2}} + V_\lambda\chi_n, \\ \tilde{V}_g &\equiv -\frac{\hbar^2}{2m}\left(\frac{3}{16\gamma^2}\gamma^{ik}(\partial_i\gamma)(\partial_k\gamma) - \frac{1}{4\gamma}\gamma^{ik}\partial_i(\partial_k\gamma)\right), \\ V_g' &\equiv -\frac{\hbar^2}{2m}\left(\frac{3}{16\Gamma^2}(\partial_3\Gamma)^2 - \frac{1}{4\Gamma}\partial_3{}^2\Gamma\right), \end{aligned} \tag{14}$$

where the relation $\partial_i\gamma^{ik} = 0$ is employed during derivation. Because of the strong confinement of the squeezing potential V_λ, the energy scale of E_n is much larger than that of E_s. Thus, the normal part χ_n in generally invariant in the eigen-states around the ground state, and the surface part χ_s is noteworthy to characterize the behaviors of the particle on the surface.

In the equation for χ_s, besides the Coriolis and centrifugal terms, there are two emerging terms $\tilde{V}_g$ and V_g', which are effective potentials from surface geometry and relativity. Compared with the case on stationary surface, it can be concluded that the potential V_g' is a relativity-corrected geometric potential. When the surface is not rotated, V_g' would become the classical geometric potential in literatures [32, 33]. Differently, the potential $\tilde{V}_g$ is a novel term, and has not been observed in the stationary case. Based on the form of $\tilde{V}_g$, the potential $\tilde{V}_g$ represents the interplay of the intrinsic Gaussian curvature and the geodesic curvature of the surface. This reflects that the rotational motion introduces some new physics into the quantum systems.

According to the typical thin-layer quantization formalism [29, 30, 34], the surface wave function χ_s should be further normalized as $\chi_s' = \gamma^{-1/4}\chi_s$, which produces a more complicated eigen-equation,

$$\begin{aligned} E_s\chi_s' &= -\frac{\hbar^2}{2m}\gamma^{ik}\left[\partial_i + \frac{1}{4\gamma}(\partial_i\gamma)\right]\left[\partial_k + \frac{1}{4\gamma}(\partial_k\gamma)\right]\chi_s' \\ &\quad + (\tilde{V}_g + V_g')\chi_s' \\ &\quad - \frac{1}{2}\gamma_{ab}\omega^a\hat{L}^b\chi_s' + \frac{m}{2}\gamma_{ab}V^aV^b\chi_s'. \end{aligned} \tag{15}$$

Comparing the eigen equations for both χ_s and χ_s' (namely, equations (14) and (15)), both the surface Schrödinger equations can describe the quantum dynamics of a spin-less particle bounded to the rotating curved surface with the effective potentials V_g', $\tilde{V}_g$, Coriolis effect and centrifugal potential. Therefore, it is possible to establish a mapping between the energy spectrum related to χ_s and to χ_s'. These two equations are equivalent in this sense. For simplicity, in the following we will take equation (14) to analyze the behaviors of particles constrained on various rotating surfaces.

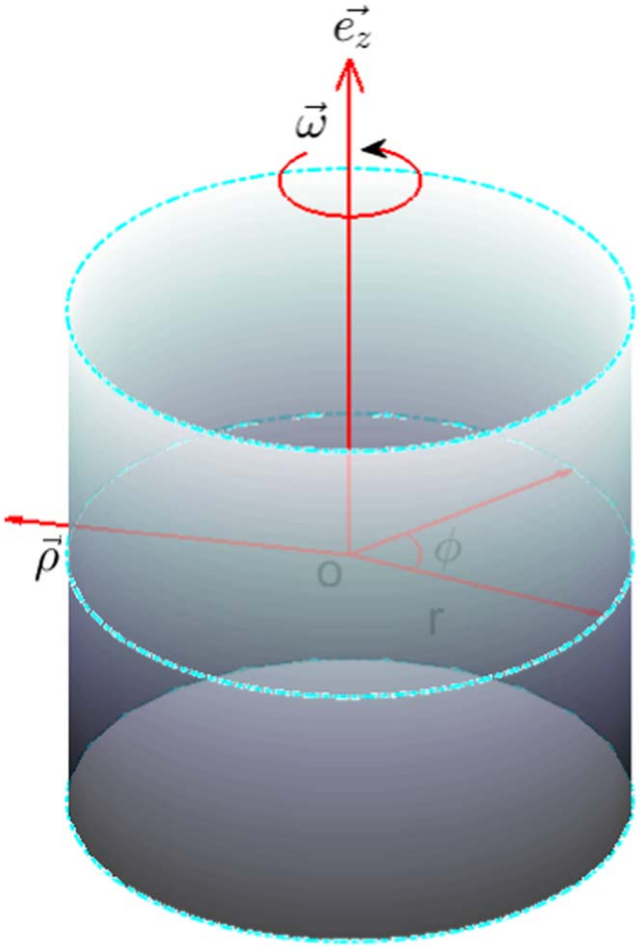

Figure 1. A rotating cylinder with radius r and its coordinate system (ϕ, z, ρ).

4. Rotating cylinder surface

The cylinder surface is a simple surface bending along one direction. Here, we consider the rotation around its axis. In the cylindrical coordinate system (ϕ, z, ρ), the line element in Minkowski space is given by:

$$\mathrm{d}s^2 = -c^2\mathrm{d}t^2 + \rho^2\mathrm{d}\phi^2 + \mathrm{d}z^2 + \mathrm{d}\rho^2. \tag{16}$$

Assuming that the cylinder has its radius r and rotates around the axis $\vec{e}_z$ with angular velocity $\vec{\omega}$, as sketched in figure 1. We now introduce the rotating frame of reference:

$$\begin{aligned} t &= t', \\ \rho &= \rho', \\ z &= z', \\ \phi &= \phi' + \omega t'. \end{aligned} \tag{17}$$

Substituting the rotating coordinates into equation (16) yields

$$\begin{aligned} \mathrm{d}s^2 = -c^2\mathrm{d}t'^2\left(1 - \frac{\rho'^2\omega^2}{c^2}\right) + \rho'^2\mathrm{d}\phi'^2 + \mathrm{d}z'^2 \\ + \mathrm{d}\rho'^2 + 2\frac{\omega\rho'^2}{c}c\mathrm{d}t'\mathrm{d}\phi'. \end{aligned} \tag{18}$$

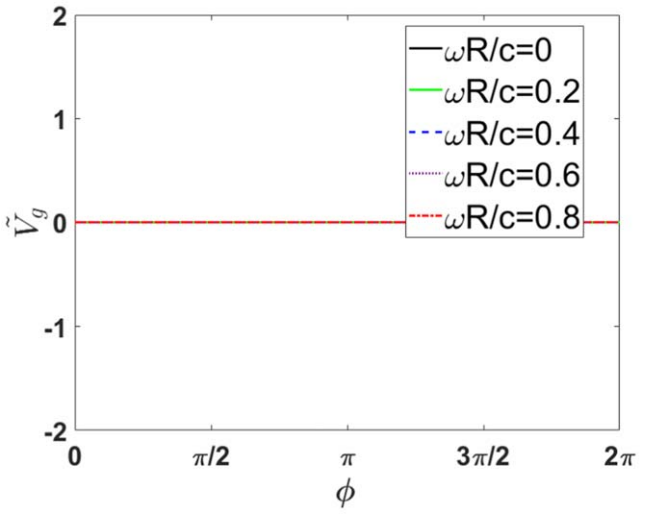

Figure 2. $\tilde{V}_g$ versus ϕ for the cases of r = 1 and $\frac{\omega r}{c} = 0$, 0.2, 0.4, 0.6, 0.8 on the rotating cylinder. Here, $\frac{\hbar^2}{2m}$ is taken as a unit.

Dropping the prime on the coordinates for simplicity, the proper length on the rotating cylinder (namely in the form of equation (4)) can be deduced based on equation (18) with the condition $\mathrm{d}\rho = 0$ as

$$\mathrm{d}l^2 = u_c^2(r)\mathrm{d}\phi^2 + \mathrm{d}z^2. \tag{19}$$

with $u_c(r) = r\Big/\sqrt{1 - \Omega_1^2}$, and $\Omega_1 = \omega r/c$. Therefore, the covariant components of metric tensor γ_{ik} are:

$$\gamma_{\phi\phi} = u_c^2(r),\ \gamma_{zz} = 1,\ \gamma_{\phi z} = \gamma_{z\phi} = 0, \tag{20}$$

and of the metric tensor Γ_{ab} as:

$$\begin{aligned} &\Gamma_{\phi\phi} = u_c^2(r + q_3), \\ &\Gamma_{\phi z} = \Gamma_{\phi q^3} = \Gamma_{z\phi} = \Gamma_{zq^3} = \Gamma_{q^3\phi} = \Gamma_{q^3 z} = 0, \\ &\Gamma_{zz} = \Gamma_{q^3 q^3} = 1, \end{aligned} \tag{21}$$

and the determinant $\Gamma = u_c^2(r + q^3)$. Note that in the cylindrical coordinate, $\vec{\omega} = (0, \omega, 0)$, $\vec{r} = (0, z, r)$. Now the Hamiltonian reads:

$$H = -\frac{\hbar^2}{2m}\Delta + \mathrm{i}\frac{\hbar}{2}\frac{\omega r}{u_c}\partial_\phi + \frac{1}{2}m\omega^2 r^2 + V_\lambda. \tag{22}$$

Following the above results, here we factorize the wave function as $\psi(\phi, z, q^3) = \Gamma^{-1/4}\chi(\phi, z, q^3)$ to derive an equation without terms which contain $\partial_a\psi$, which is well in line with the thin-layer quantization formalism [29–31]. According to the proper length of equation (19), we expand equation (12) in the cylindrical coordinate as:

$$E\chi = -\frac{\hbar^2}{2m}\left(\frac{1}{u_c^2}\partial_\phi^2 + \partial_z^2 + \partial_{q^3}^2\right)\chi + V_g'\chi + V_\lambda\chi. \tag{23}$$

In this equation, the effective potential $\tilde{V}_g = 0$, since the derivative ∂_ϕ or ∂_ϕ^2 cannot bring anything from the metric tensor, as shown in figure 2. Besides, the potential V_g' has the

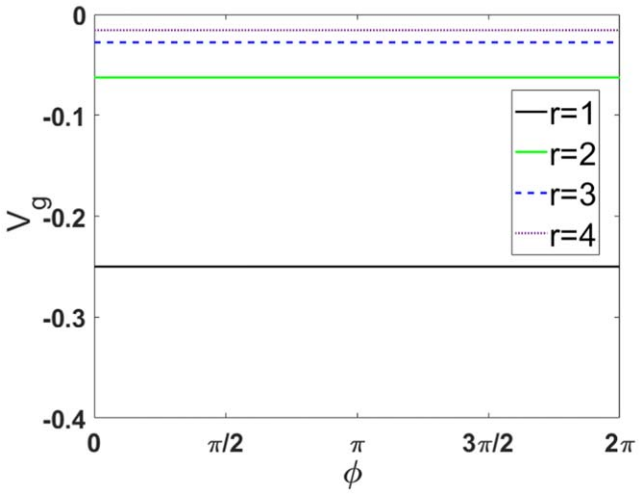

Figure 3. V_g versus ϕ for the cases of r = 1, 2, 3, 4 on the rotating cylinder. Here, $\frac{\hbar^2}{2m}$ is taken as a unit.

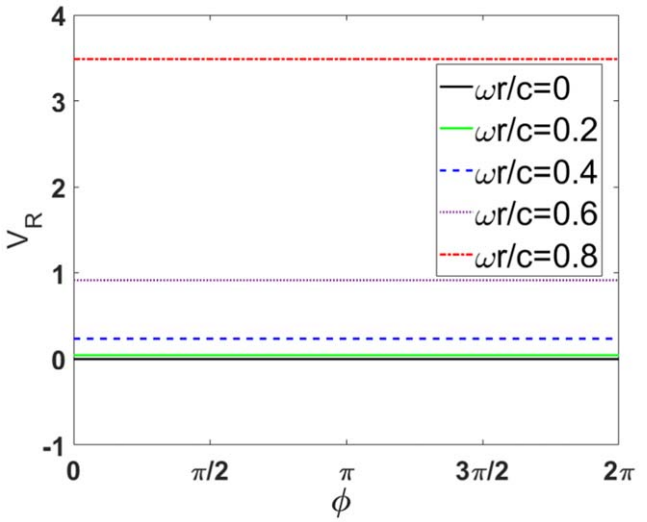

Figure 4. V_R versus ϕ for the cases of r = 1 and $\frac{\omega r}{c} = 0$, 0.2, 0.4, 0.6, 0.8 on the rotating cylinder. Here, $\frac{\hbar^2}{2m}$ is taken as a unit.

following form:

$$V_g' = -\frac{\hbar^2}{8mr^2}(1 - 4\Omega_1^2 - 9\Omega_1^4 - 14\Omega_1^6 - 24\Omega_1^8). \quad (24)$$

It is easy to find that $V_g = V_g'(\omega = 0) = -\hbar^2/8mr^2$ is consistent with the geometric potential on a stationary cylinder surface (as described in figure 3). Meanwhile, the rest part $V_R = V_g' - V_g$ reflects the contribution of relativistic effect to geometric potential (as sketched in figure 4). Obviously, V_g', V_g and V_R are all independent of ϕ and z, which indicates that the potentials are constants on the cylinder surface, and would only shift the energy spectra and do not affect the energy gaps. On the other hand, the potential V_g and V_R all depend on the radius r, and increase for larger radius r. This kind of dependence on r outlines the preference to thin cylinder. The difference of the potentials V_g and V_R is their signs. Thus, these potentials would shift the spectrum in different directions, and may compensate with each other. More importantly, the relativistic correction V_R is a function of rotation frequency ω. It is possible to enlarge the potential V_R by speeding up the rotation. Especially, when $\Omega_1 = \omega r/c$ turns to 0.4, V_g and V_R may cancel out each other, and V_g' becomes 0. It is worth noting that when considering a rotating disc with thickness, in addition to the $\tilde{V}_g$ mentioned in [12], there are effects of V_g' on the side surface.

With the separation $\chi(\phi, z, q^3) = \chi_s(\phi, z)\chi_n(q^3)$, we can decouple the Schrödinger equation into a surface component and a normal component as

$$\begin{aligned} E_s\chi_s &= -\frac{\hbar^2}{2m}\left(\frac{1}{u_c^2}\partial_\phi^2 + \partial_z^2\right)\chi_s + V_g'\chi_s \\ &+ \mathrm{i}\frac{\hbar\omega r}{2u_c}\partial_\phi\chi_s + \frac{1}{2}m\omega^2 r^2\chi_s, \\ E_n\chi_n &= -\frac{\hbar^2}{2m}\partial_{q^3}^2\chi_n + V_\lambda\chi_n. \end{aligned} \quad (25)$$

To solve the effective Schrödinger equation for the surface part χ_s, we introduce the ansatz for the wave function:

$$\chi_s(\phi, z) = \mathrm{e}^{\mathrm{i}N\phi}\Phi(z), \quad (26)$$

where N represents quantized angular momentum [12]. This leads to the following Schrödinger equation:

$$-\frac{\hbar^2}{2m}\partial_z^2\Phi + V_T^c\Phi = E\Phi, \quad (27)$$

in which V_T^c represents the total effective potential:

$$\begin{aligned} V_T^c &= -\frac{\hbar^2}{2mr^2}\textstyle\sum_{n=0}^4 \Omega_1^{2n} Z_n^c + \frac{1}{2}m\omega^2 r^2, \\ Z_0^c &= \frac{1}{4} - N^2 + Lr^2, \\ Z_1^c &= -1 + N^2 - \frac{Lr^2}{2}, \\ Z_2^c &= -\frac{9}{4} - \frac{Lr^2}{8}, \\ Z_3^c &= -\frac{7}{2} - \frac{Lr^2}{16}, \\ Z_4^c &= -6, \end{aligned} \quad (28)$$

with $L = mN\omega/\hbar$. Note that $V_{T,N}^c(r) = V_{T,-N}^c(r)$ for $\Omega_1 = 0$, namely, the rotation breaks the degeneracy in N. Additionally, in this potential, the Coriolis effect and the centrifugal term are included.

5. Rotating sphere surface

A sphere is another typical isotropic geometric surface. Here, we consider the rotation around any a diameter of the sphere. In the spherical coordinate system (θ, ϕ, ρ), the line element in Minkowski space is given by,

$$\mathrm{d}s^2 = -c^2\mathrm{d}t^2 + \rho^2\mathrm{d}\theta^2 + \rho^2\sin^2\theta\mathrm{d}\phi^2 + \mathrm{d}\rho^2. \quad (29)$$

Assuming that a sphere has a radius r, and rotates around the axis $\vec{e}_z$ through the spheric center with constant angular velocity

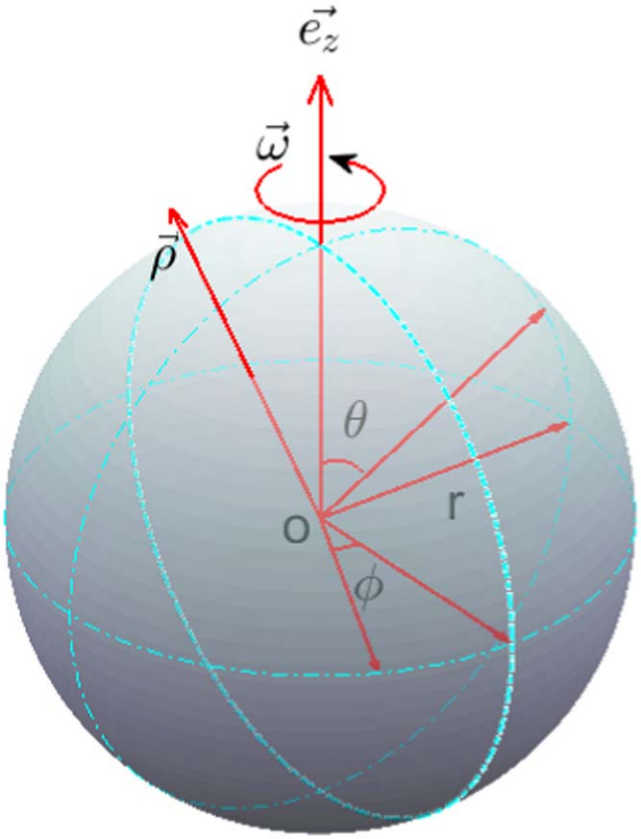

Figure 5. A rotating sphere with radius r and its coordinate system (θ, ϕ, ρ).

$\vec{\omega}$ (as shown in figure 5). Considering the transformation from the stationary to the rotating coordinate system [11], we have

$$\begin{aligned} t &= t', \\ \rho &= \rho', \\ \theta &= \theta', \\ \phi &= \phi' + \omega t', \end{aligned} \tag{30}$$

where the primed terms are defined in the rotating coordinate system. Substituting the equation (30) into equation (29), the line element in the rotating frame is rewritten as:

$$\begin{aligned} \mathrm{d}s^2 = &-c^2\mathrm{d}t'^2\left(1 - \frac{\rho'^2\sin^2\theta'\omega^2}{c^2}\right) + \rho'^2\sin^2\theta'\mathrm{d}\phi'^2 \\ &+\rho'^2\mathrm{d}\theta'^2 + \mathrm{d}\rho'^2 + 2\frac{\omega\rho'^2\sin^2\theta'}{c}c\mathrm{d}t'\mathrm{d}\phi'. \end{aligned} \tag{31}$$

In what follows we drop the prime on the coordinates for simplicity. The proper length on the rotating sphere surface (namely in equation (4)) can be deduced based on equation (31) with the condition $\mathrm{d}\rho = 0$ as

$$\mathrm{d}l^2 = r^2\mathrm{d}\theta^2 + u_s^2(r, \theta)\mathrm{d}\phi^2, \tag{32}$$

where $u_s(r, \theta) = r\sin\theta/\sqrt{1 - \Omega_2^2}$, and $\Omega_2 = \omega r\sin\theta/c$. Obviously, the covariant components of the metric tensor γ_{ik} are:

$$\gamma_{\theta\theta} = r^2,\ \gamma_{\phi\phi} = u_s^2(r, \theta),\ \gamma_{\theta\phi} = \gamma_{\phi\theta} = 0, \tag{33}$$

and of the metric tensor Γ_{ab} as

$$\begin{aligned} &\Gamma_{\theta\theta} = (r + q_3)^2,\ \Gamma_{\phi\phi} = u_s^2(r + q_3, \theta),\ \Gamma_{q_3q_3} = 1, \\ &\Gamma_{\theta\phi} = \Gamma_{\theta q_3} = \Gamma_{\phi\theta} = \Gamma_{\phi q_3} = \Gamma_{q_3\theta} = \Gamma_{q_3\phi} = 0, \end{aligned} \tag{34}$$

and the determinant $\Gamma = (r + q_3)^2u_s^2(r + q_3, \theta)$. Note that in the spherical coordinate, $\vec{\omega} = (-\omega\sin\theta, 0, \omega\cos\theta)$, $\vec{r} = (0, 0, r)$. Thus, the Hamiltonian for a spin-less particle on the rotating sphere surface reads:

$$H = -\frac{\hbar^2}{2m}\nabla^2 + \mathrm{i}\frac{\hbar\omega r\sin\theta}{2u_s}\partial_\phi + \frac{m\omega^2r^2\sin^2\theta}{2} + V_\lambda. \tag{35}$$

Similarly, we introduce the wave function $\psi = \Gamma^{-1/4}\chi$. According to the proper length equation (32), the equation (12) can be expanded as:

$$\begin{aligned} E\chi = &-\frac{\hbar^2}{2m}\left(\frac{1}{r^2}\partial_\theta^2 + \frac{1}{u_s^2}\partial_\phi^2 + \partial_{q_3}^2\right)\chi \\ &+ (\tilde{V}_g + V_g')\chi + \mathrm{i}\frac{\hbar\omega r\sin\theta}{2u_s}\partial_\phi\chi \\ &+ \frac{1}{2}m\omega^2r^2\sin^2\theta\chi + V_\lambda\chi, \end{aligned} \tag{36}$$

where $\tilde{V}_g$ and V_g' are the effective potentials.

The potential $\tilde{V}_g$ stems from the intrinsic Gaussian curvature of the surface, $K = -\partial_\theta^2u_s/r^2u_s$, and the geodesic curvature of the $\phi-$curve, $K_g = \partial_\theta u_s/ru_s$ as

$$\tilde{V}_g = -\frac{\hbar^2}{2m}\left(\frac{K_g^2}{4} + \frac{K}{2}\right) = -\frac{\hbar^2}{2mr^2}\sum_{n=0}^{4}\Omega_2^{2n}S_n, \tag{37}$$

where the factors S_n are defined as

$$\begin{aligned} S_0 &= \frac{1}{2} + \frac{\cot^2\theta}{4}, \\ S_1 &= 1 + \cot^2\theta\left(\frac{r^2}{2} - 1\right) - \frac{1}{2\sin^2\theta}, \\ S_2 &= \frac{3}{2} + \cot^2\theta\left(\frac{3r^2}{4} - 2\right) - \frac{1}{\sin^2\theta}, \\ S_3 &= 2 + \cot^2\theta(r^2 - 3) - \frac{3}{2\sin^2\theta}, \\ S_4 &= -4\cot^2\theta - \frac{2}{\sin^2\theta}. \end{aligned} \tag{38}$$

The properties of $\tilde{V}_g$ is shown in figure 6. It is observed that from the equator to the poles, the potential is divergent and always negative. Besides, $\tilde{V}_g$ takes its extreme values at $\theta = \pi/2$, these values have the following form:

$$(\tilde{V}_g)_{\max/\min} = -\frac{\hbar^2}{2mr^2}\frac{1}{2}(1 + \Omega_2^2 + \Omega_2^4 + \Omega_2^6 - 4\Omega_2^8). \tag{39}$$

It is worth noting that when the radius $r = 1$, the faster rotation would split the extremum into two, appearing around $\theta = \pi/4$ and $\theta = 3\pi/4$, respectively. However, as the radius r increase, the rotation effect is negligible.

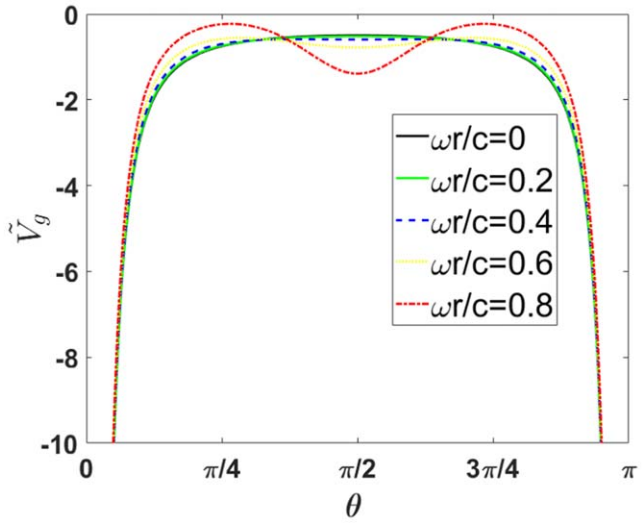

Figure 6. $\tilde{V}_g$ versus θ for the cases of r = 1 and $\frac{\omega r}{c} = 0$, 0.2, 0.4, 0.6, 0.8 on the rotating sphere. Here, $\frac{\hbar^2}{2m}$ is taken as a unit.

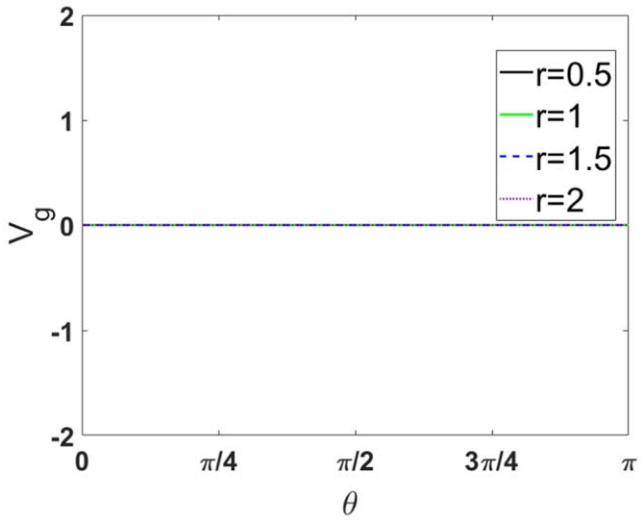

Figure 7. V_g versus θ for the cases of r = 0.5, 1, 1.5, 2 on the rotating sphere. Here, $\frac{\hbar^2}{2m}$ is taken as a unit.

The geometrical potential V_g' has the following form:

$$V_g' = \frac{\hbar^2}{8mr^2}(6{\Omega_2}^2 + 11{\Omega_2}^4 + 16{\Omega_2}^6 + 21{\Omega_2}^8 - 4{\Omega_2}^{10}), \tag{40}$$

Clearly, for the case without rotation, the geometric potential $V_g = V_g'(\omega = 0)$ is 0, (as shown in figure 7), which is consistent with the previous research [32]. The correction term $V_R = V_g' - V_g$ represents the relativity-induced geometric potential, which is described in figure 8. It is obvious that the potential V_R is always positive, and acts as a barrier on the sphere. The faster the frequency, the higher the barrier is. Similar to the potential $\tilde{V}_g$, the maximal values of V_g' is located at $\theta = \pi/2$. The correponding maximum has the following

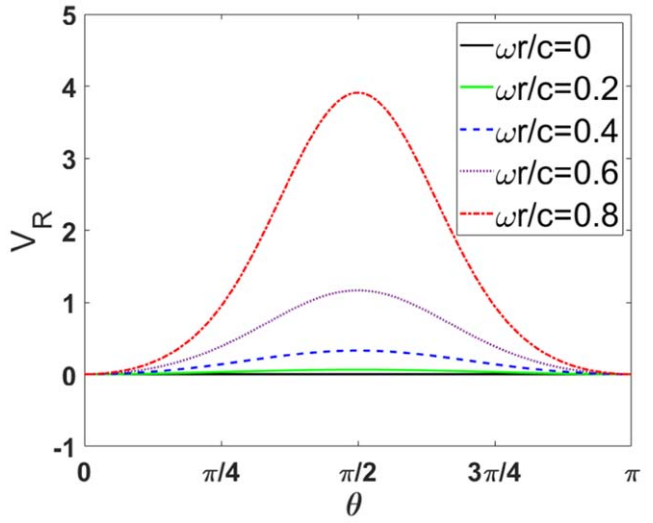

Figure 8. V_R versus θ for the cases of r = 1 and $\frac{\omega r}{c} = 0$, 0.2, 0.4, 0.6, 0.8 on the rotating sphere. Here, $\frac{\hbar^2}{2m}$ is taken as a unit.

form:

$$(V_g')_{\max} = \frac{\hbar^2}{8mr^2}(6\Omega_1^2 + 11\Omega_1^4 + 16\Omega_1^6 + 21\Omega_1^8 - 4\Omega_1^{10}). \tag{41}$$

Compared to the potential $\tilde{V}_g$, with certain $r = 1$, for $\omega r/c > 0.5$, V_g' may compensate or even overwrite the local minimum of $\tilde{V}_g$ around $\pi/2$.

Together with various effects, these two geometric potentials generally bias towards the poles of the sphere. It suggests the particle is more likely to appear at the poles. This mainly comes from the relativity-corrected potential V_g'. Together with these kind of potentials, the distribution of particle on the surface is not uniform. The quantum confinement would enhance the energy gaps between states.

Suppose that the wave function $\chi(\theta, \phi, q^3)$ can be separated into $\chi(\theta, \phi, q^3) = \chi_s(\theta, \phi)\chi_n(q_3)$ with $\chi_s(\theta, \phi)$ and $\chi_n(q^3)$ standing for the surface component and the normal component, respectively. The equation (36) can be separated into a surface and a normal Schrödinger equation:

$$\begin{aligned} E_s\chi_s &= -\frac{\hbar^2}{2m}\left(\frac{1}{r^2}\partial_\theta^2 + \frac{1}{u_s^2}\partial_\phi^2\right)\chi_s + (\tilde{V}_g + V_g')\chi_s \\ &+ \mathrm{i}\frac{\hbar\omega r\sin\theta}{2u_s}\partial_\phi\chi_s + \frac{1}{2}m\omega^2 r^2\sin^2\theta\chi_s, \\ E_n\chi_n &= -\frac{\hbar^2}{2m}\partial_{q^3}^2\chi_n + V_\lambda\chi_n. \end{aligned} \tag{42}$$

We focus on the surface component and make the following ansatz for the wave function:

$$\chi_s(\theta, \phi) = e^{\mathrm{i}N\phi}\Phi(\theta). \tag{43}$$

This leads to the following Schrödinger equation:

$$-\frac{\hbar^2}{2mr^2}\partial_\theta^2\Phi + V\Phi = E\Phi. \tag{44}$$

Let $r^2E = E'$, $r^2V = V_t$, then we have

$$-\frac{\hbar^2}{2m}\partial_\theta^2\Phi + V_T^s\Phi = E'\Phi, \tag{45}$$

where V_T^s represents the total effective potential:

$$\begin{aligned}
V_t &= -\frac{\hbar^2}{2m}\sum_{n=0}^{5}\Omega_2^{2n}Z_n^S + \frac{1}{2}m\omega^2r^4\sin^2\theta,\\
Z_0^S &= \frac{1}{2} + \frac{\cot^2\theta}{4} + Lr^2 - \frac{N^2}{\sin^2\theta},\\
Z_1^S &= -\frac{1}{2} + \cot^2\theta\left(\frac{r^2}{2} - 1\right) - \frac{1-2N^2}{2\sin^2\theta} - \frac{Lr^2}{2},\\
Z_2^S &= -\frac{5}{4} + \cot^2\theta\left(\frac{3r^2}{4} - 2\right) - \frac{1}{\sin^2\theta} - \frac{Lr^2}{8},\\
Z_3^S &= -2 + \cot^2\theta(r^2 - 3) - \frac{3}{2\sin^2\theta} - \frac{Lr^2}{16},\\
Z_4^S &= -\frac{21}{4} - 4\cot^2\theta - 2\sin^2\theta,\\
Z_5^S &= 1.
\end{aligned} \tag{46}$$

In the effective potential, the Coriolis term is included as $-\hbar^2L/2m(1 - \Omega_2^2/2 - \Omega_2^4/8 - \Omega_2^6/16)$, in which the rotation is coupled to the angular momentum and shifts the energy spectrum, as indicated in [28]. The role of the zero-order term is opposite to that of the higher-order terms.

6. Rotating torus surface

Besides the cylinder and sphere, the torus is a surface with different topology. We consider the rotation of a torus surface along the symmetric axis perpendicular to the center plane. In the reference system (θ, ϕ, ρ), the line element in Minkowski space is given by:

$$\mathrm{d}s^2 = -c^2\mathrm{d}t^2 + \rho^2\mathrm{d}\theta^2 + (R + \rho\sin\theta^2)^2\,\mathrm{d}\phi^2 + \mathrm{d}\rho^2. \tag{47}$$

Assuming that the torus has the radius R, the radius of the tube is r, and the torus rotates around $\vec{e_z}$ (as shown in figure 9). After making the rotation transformation:

$$\begin{aligned}
t &= t',\\
\rho &= \rho',\\
\theta &= \theta',\\
\phi &= \phi' + \omega t',
\end{aligned} \tag{48}$$

the line element in equation (47) is turned to:

$$\begin{aligned}
\mathrm{d}s^2 = &-c^2\mathrm{d}t'^2\left(1 - \frac{(R + \rho'\sin\theta')^2\,\omega^2}{c^2}\right)\\
&+ \rho'^2\mathrm{d}\theta'^2 + \mathrm{d}\rho'^2\\
&+ (R + \rho'\sin\theta')^2\,\mathrm{d}\phi'^2\\
&+ \frac{2\omega(R + \rho'\sin\theta')^2}{c}c\mathrm{d}t'\mathrm{d}\phi'.
\end{aligned} \tag{49}$$

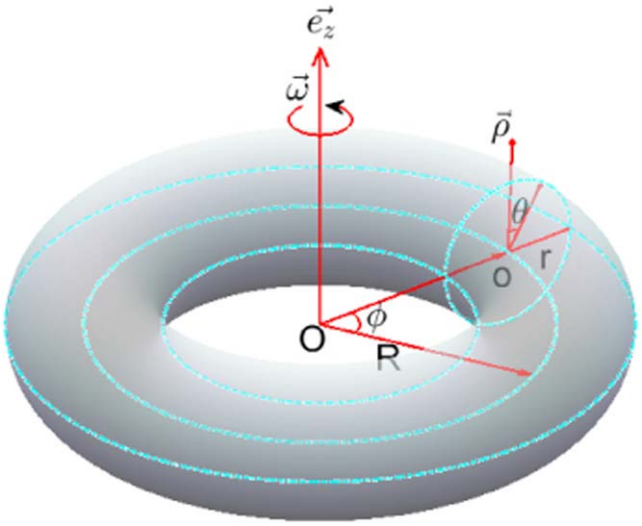

Figure 9. A rotating torus of radius r and its coordinate system (θ,ϕ, ρ). r is the radius of the tube, R is the radius of the central circle.

In what follows we will drop the prime on the coordinate. The proper length on the rotating torus (namely in the form of equation (4)) can be deduced based on equation (49) as

$$\mathrm{d}l^2 = r^2\mathrm{d}\theta^2 + u_t^2(r,\,\theta)\mathrm{d}\phi^2, \tag{50}$$

where $u_t(r,\,\theta) = a\Big/\sqrt{1 - \Omega_3^2}$, $a = R + r\sin\theta$, $\Omega_3 = \omega a/c$. Accordingly, the covariant components of metric γ_{ik} are:

$$\gamma_{\theta\theta} = r^2,\ \gamma_{\phi\phi} = u_t^2(r,\,\theta),\ \gamma_{\theta\phi} = \gamma_{\phi\theta} = 0, \tag{51}$$

and of metric tensor Γ_{ab} are

$$\begin{aligned}
&\Gamma_{\theta\theta} = (r + q^3)^2,\ \Gamma_{\phi\phi} = u_t^2(a_q,\,\theta),\ \Gamma_{q^3q^3} = 1\\
&\Gamma_{\theta\phi} = \Gamma_{\theta q^3} = \Gamma_{\phi\theta} = \Gamma_{\phi q^3} = \Gamma_{q^3\theta} = \Gamma_{q^3\phi} = 0,
\end{aligned} \tag{52}$$

and the determinant $\Gamma = (r + q^3)^2u_t^2(a_q,\,\theta)$, where $a_q = a + q^3\sin\theta$. Note that in the toroidal coordinate, $\vec{\omega} = (-\omega\sin\theta,\,0,\,\omega\cos\theta)$, $\vec{r} = (R\cos\theta,\,0,\,R\sin\theta + r)$. Now the Hamiltonian reads:

$$H = -\frac{\hbar^2}{2m}\Delta + \mathrm{i}\frac{\hbar\omega a}{2u_t}\partial_\phi + \frac{1}{2}m\omega^2a^2 + V_\lambda. \tag{53}$$

Similar to other surfaces, we introduce the wave function as $\psi(\theta,\,\phi,\,q^3) = \Gamma^{-1/4}\chi(\theta,\,\phi,\,q^3)$. According to the proper length (equation (50)), we can calculate the equation (12) in the toroidal coordinate as:

$$\begin{aligned}
E\chi = &-\frac{\hbar^2}{2m}\left(\frac{1}{r^2}\partial_\theta^2 + \frac{1}{u_t^2}\partial_\phi^2 + \partial_{q^3}^2\right)\chi\\
&+ (\tilde{V}_g + V_g')\chi + \mathrm{i}\frac{\hbar\omega a}{2u_t}\partial_\phi\chi_s\\
&+ \frac{1}{2}m\omega^2a^2\chi + V_\lambda\chi,
\end{aligned} \tag{54}$$

where $\tilde{V}_g$ and V_g' are effective potentials.

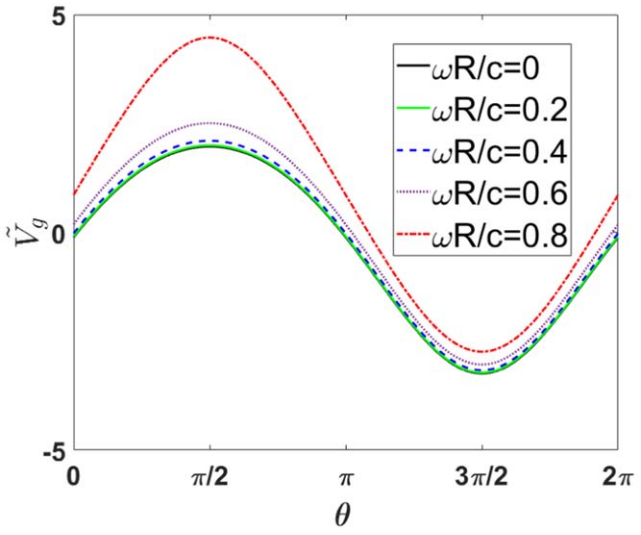

Figure 10. The geometric potential $\tilde{V}_g$ versus θ for the cases of R = 1, r = 0.2 and $\frac{\omega R}{c} = 0$, 0.2, 0.4, 0.6, 0.8 on the rotating torus. Here, $\frac{\hbar^2}{2m}$ is taken as a unit.

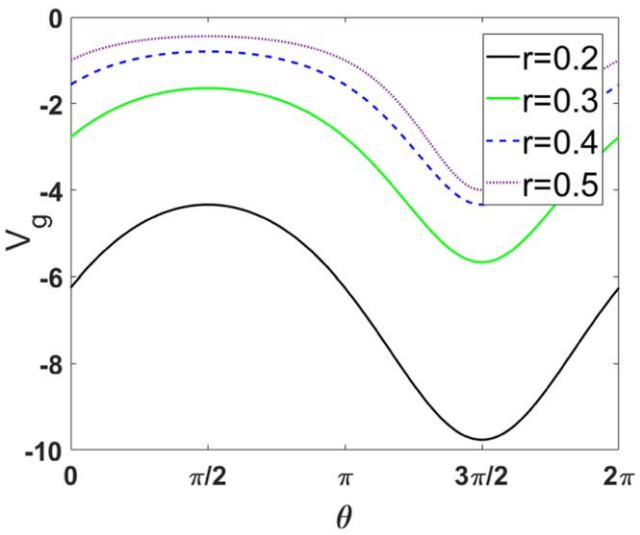

Figure 11. V_g versus θ for the cases of R = 1, r = 0.2, 0.3, 0.4, 0.5 on the rotating torus. Here, $\frac{\hbar^2}{2m}$ is taken as a unit.

The potential $\tilde{V}_g$ has the form:

$$\tilde{V}_g = -\frac{\hbar^2}{2ma^2}\sum_{n=0}^{5}\Omega_3^{2n}T_n,$$
$$T_0 = \frac{\sin^2\theta}{2Q} + \frac{\cos^2\theta}{4},\ T_1 = \frac{Q}{2} - \cos^2\theta,$$
$$T_2 = \frac{Q}{2} - \frac{5\cos^2\theta}{4},\ T_3 = \frac{Q}{2} - \frac{3\cos^2\theta}{2},$$
$$T_4 = \frac{Q}{2} - 3\cos^2\theta,\ T_5 = 2\cos^2\theta, \tag{55}$$

where $Q = r\sin\theta/a$. Here, $\tilde{V}_g$ is composed of the intrinsic Gaussian curvature term (related to $\partial^2 u_t/\partial\theta^2$) and the geodesic curvature term (related to $(\partial u_t/\partial\theta)^2$) of the rotating torus. The properties of this term is shown in figure 10. It is observed that $\tilde{V}_g$ increases monotonically with rotational frequency. Besides, it is found that the relation of $\tilde{V}_g$ versus θ is not linear. The potential has opposite signs in the interval [0, π] and [π, 2π], namely, $\tilde{V}_g$ appears as attractive on the inside surface and as repulsive on the outside, compared to the free particle.

The potential V_g' has the following form:

$$V_g' = -\frac{\hbar^2}{2mr^2}\sum_{n=0}^{5}\Omega_3^{2n}\Xi_n,$$
$$\Xi_0 = \frac{R^2}{4a^2},\ \Xi_1 = \frac{Q}{2} + \frac{Q^2}{c^2},$$
$$\Xi_2 = \frac{Q}{2} + \frac{Q^2}{4} + \frac{2Q^2}{c^2},\ \Xi_3 = \frac{Q}{2} + \frac{Q^2}{2} + \frac{3Q^2}{c^2},$$
$$\Xi_4 = \frac{Q}{2} + \frac{3Q^2}{4} + \frac{4Q^2}{c^2},\ \Xi_5 = Q^2. \tag{56}$$

Here, the potential V_g' is composed of the contribution without rotation ($V_g = -\hbar^2R^2/8ma^2r^2$) and the rotation-related

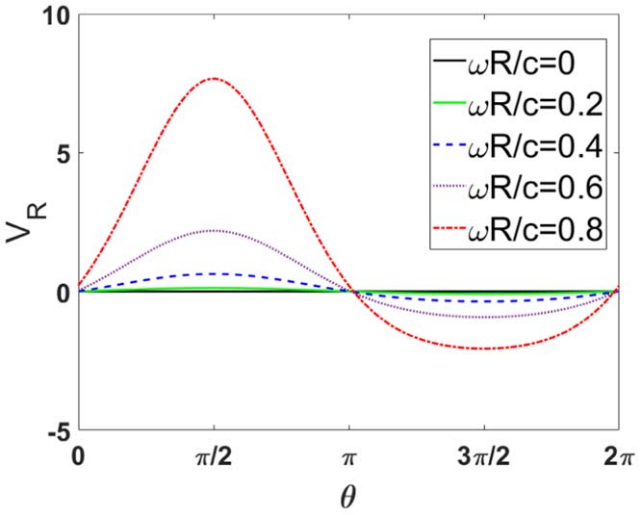

Figure 12. V_R versus θ for the cases of R = 1, r = 0.2 and $\frac{\omega R}{c} = 0$, 0.2, 0.4, 0.6, 0.8 on the rotating torus. Here, $\frac{\hbar^2}{2m}$ is taken as a unit.

relativistic effect $V_R = V_g' - V_g$. The terms V_g and V_R versus θ are given in figures 11 and 12, respectively. Clearly, the potential V_g is always negative. Besides, for a thicker tube with a larger radius r, the effect of V_g would become weaker. This is consistent with the picture that V_g is generated from surface curvature. For a certain torus, the potential V_g for the case $\theta \in [\pi, 2\pi]$ is generally smaller than that when $\theta \in [0, \pi]$, showing the similar trend as those for $\tilde{V}_g$. At the same time, it can be observed through the figure 12 that the relationship of V_R versus θ is also similar to the variation of $\tilde{V}_g$. The variation of V_R means that the rotation raises up (suppresses) the geometric potential on the inner (outer) part of torus (corresponding to $\theta \in [0, \pi]([\pi, 2\pi])$). This kind of effect would be enhanced for faster rotation. Quantitatively, the geometric

potential V_g' takes its maximum at $\theta = \pi/2$ as

$$
\begin{aligned}
&(V_g')_{\max} = -\frac{\hbar^2}{2ma^{\dagger 2}}\sum_{n=0}^{5}\Omega_3^{\dagger 2n}\Xi_n^{\dagger},\\
&\Xi_0^{\dagger} = \frac{R^2}{4r^2},\ \Xi_1^{\dagger} = -\frac{a^{\dagger}}{2r} - \frac{1}{c^2},\\
&\Xi_2^{\dagger} = -\frac{a^{\dagger}}{2r} - \frac{1}{4} - \frac{2}{c^2},\ \Xi_3^{\dagger} = -\frac{a^{\dagger}}{2r} - \frac{1}{2} - \frac{3}{c^2},\\
&\Xi_4^{\dagger} = -\frac{a^{\dagger}}{2r} - \frac{3}{4} - \frac{4}{c^2},\ \Xi_5^{\dagger} = -1,
\end{aligned}
\tag{57}
$$

where $a^{\dagger} = R + r$, and $\Omega_3^{\dagger} = \omega a^{\dagger}/c$, the minimum at $\theta = 3\pi/2$ as:

$$
\begin{aligned}
&(V_g')_{\min} = -\frac{\hbar^2}{2ma^{\ddagger 2}}\sum_{n=0}^{5}\Omega_3^{\ddagger 2n}\Xi_n^{\ddagger}\\
&\Xi_0^{\ddagger} = \frac{R^2}{4r^2},\ \Xi_1^{\ddagger} = \frac{a^{\ddagger}}{2r} - \frac{1}{c^2}\\
&\Xi_2^{\ddagger} = \frac{a^{\ddagger}}{2r} - \frac{1}{4} - \frac{2}{c^2},\ \Xi_3^{\ddagger} = \frac{a^{\ddagger}}{2r} - \frac{1}{2} - \frac{3}{c^2},\\
&\Xi_4^{\ddagger} = \frac{a^{\ddagger}}{2r} - \frac{3}{4} - \frac{4}{c^2},\ \Xi_5^{\ddagger} = -1,
\end{aligned}
\tag{58}
$$

where $a^{\ddagger} = R - r$, and $\Omega_3^{\ddagger} = \omega a^{\ddagger}/c$. These results implie that the extreme values depend not only on the intrinsic curvature of the surface, but also on the connection between the surface curvature and the special relativity. Particularly, the rotation widens the gap between the peak and valley, makes the particle prefer to stay near the inner side of the rotating torus and generate new bound states [6, 8, 9].

Assuming that the wave function χ satisfies $\chi(\theta, \phi, q^3) = \chi_s(\theta, \phi)\chi_n(q^3)$. We decompose the Schrödinger equation into surface and normal components:

$$
\begin{aligned}
E_s\chi_s =& -\frac{\hbar^2}{2m}\left(\frac{1}{r^2}\partial_\theta^2 + \frac{1}{u_t^2}\partial_\phi^2\right)\chi_s + (\tilde{V}_g + V_g')\chi_s\\
&+ \mathrm{i}\frac{\hbar\omega a}{2u_t}\partial_\phi\chi_s + \frac{1}{2}m\omega^2a^2\chi_s,\ E_n\chi_n\\
=& -\frac{\hbar^2}{2m}\partial_{q^3}^2\chi_n + V_\lambda\chi_n.
\end{aligned}
\tag{59}
$$

The ansatz for the surface wave function $\chi_s(\theta, \phi) = e^{\mathrm{i}N\phi}\Phi(\theta)$ turns the effective surface Schrödinger to

$$
-\frac{\hbar^2}{2mr^2}\partial_\theta^2\Phi + V\Phi = E\Phi. \tag{60}
$$

Let $r^2E = E'$, $r^2V = V_T^t$,then

$$
-\frac{\hbar^2}{2m}\partial_\theta^2\Phi + V_T^t\Phi = E'\Phi, \tag{61}
$$

where V_t represents the total effective potential:

$$
\begin{aligned}
&V_T^t = -\frac{\hbar^2}{2m}\sum_{n=0}^{5}\Omega_3^{2n}Z_n^T + \frac{1}{2}m\omega^2r^2a^2,\\
&Z_0^T = \frac{R^2}{4a^2} + \frac{Q}{2} + \frac{Q^2(\cos^2\theta - 4N^2)}{4\sin^2\theta} + Lr^2,\\
&Z_1^T = -\frac{Q}{2} - \frac{Q^2(2\cos^2\theta - 2N^2 - Q)}{2\sin^2\theta} - \frac{Q^2}{c^2} - \frac{Lr^2}{2},\\
&Z_2^T = -\frac{Q}{2} - \frac{Q^2(4\cos^2\theta + 1 - 2Q)}{4\sin^2\theta} - \frac{2Q^2}{c^2} - \frac{Lr^2}{8},\\
&Z_3^T = -\frac{Q}{2} - \frac{Q^2(2\cos^2\theta + 1 - Q)}{2\sin^2\theta} - \frac{3Q^2}{c^2} - \frac{Lr^2}{16},\\
&Z_4^T = -\frac{Q}{2} - \frac{Q^2(9\cos^2\theta + 3 - 2Q)}{4\sin^2\theta} - \frac{4Q^2}{c^2},\\
&Z_5^T = -Q^2(1 + 2\cot^2\theta).
\end{aligned}
\tag{62}
$$

In the present system, the Coriolis term $-\frac{\hbar^2}{2m}Lr^2(1 - \frac{1}{2}\Omega_3{}^2 - \frac{1}{8}\Omega_3{}^4 - \frac{1}{16}\Omega_3{}^6)$ and centrifugal potential term $\frac{1}{2}\omega^2r^2a^2$ also appear in the effective Schrödinger equation. Besides, the V_g acts as a potential well on the torus, and the rotation changes the sign of the effective potential inside and outside the torus. The results are helpful to change the band structure and manipulate the electron transport.

7. Conclusion

In this paper, we have considered quantum physics related to the rotational surface $\mathcal{S}$ in Minkowski space $\mathcal{M}$. We have proposed an approach combining the thin-layer quantization formalism with the special relativity, and derived the effective Schrödinger equation describing a spin-less particle confined to a rotating curved surface. With a proper choice of wave function, we have accomplished the separation of the effective Schrödinger equation into surface and normal parts.

To explicitly exemplify the connection between rotation and the surface geometry, we have applied the surface Schrödinger equation to a rotating cylinder, sphere and torus surfaces. The rotation offers a relativistic correction term V_R to the classical geometric potential V_g. On the other hand, a novel effective potential $\tilde{V}_g$ related to the interplay of the intrinsic Gaussian curvature and geodesic curvature of the surface resulting from the relativity appears in three examples, respectively. These potentials can effectively manipulate the transport properties of electrons bases on its ability to change the role played by potentials. Additionally, the appearance of the Coriolis effect and centrifugal potential supports that the rotating curved surfaces act on a spin-less particle with more contributions. In these special cases, the quantum behavior of particles modified by these effects can be equivalently regarded as the motion of the particle in the total effective potential.

As a potential application, the rotation can be employed to shift the energy level and generate new bound states. These results provide a prospect of possible application to design

nano-based devices by adjusting geometric parameters and rotational frequency. In the present cases, it is straightforward to find that the potential on the rotating sphere is singular, does this affect the orthogonality of the wave function? Probability density distribution on the rotating sphere is still an interesting project that needs further investigation.

Acknowledgments

This work is jointly supported by the National Nature Science Foundation of China (Grants No. 11 774 157, No. 11 934 008, No. 12 075 117, No. 51 721 001, No. 11 890 702, No. 11 625 418, No. 11 535 005, No. 11 690 030). Y-L W was funded by the Natural Science Foundation of Shandong Province of China (Grant No. ZR2020MA091).

ORCID iDs

Run Cheng https://orcid.org/0000-0003-3678-5949

References

[1] Tanda S, Tsuneta T, Okajima Y, Inagaki K, Yamaya K and Hatakenaka N 2002 *Nature* **417** 397
[2] Meyer J C, Geim A K, Katsnelson M I, Novoselov K S, Booth T J and Roth S 2007 *Nature* **446** 60
[3] Shima H, Sato M, Iiboshi K, Ghosh S and Arroyo M 2010 *Phys. Rev.* B **82** 085401
[4] Medina E, González-Arraga L A, Finkelstein-Shapiro D, Berche B and Mujica V 2015 *J. Chem. Phys.* **142** 194308
[5] Encinosa M and Etemadi B 1998 *Phys. Rev.* A **58** 77
[6] Encinosa M and Mott L 2003 *Phys. Rev.* A **68** 014102
[7] Ortix C and van den Brink J 2010 *Phys. Rev.* B **81** 165419
[8] Cheng R, Wang Y-L, Gao H-X, Zhao H, Wang J-Q and Zong H-S 2020 *J. Phys. Condes. MatterJ. Phys. Condes. Matter* **32** 025504
[9] Cheng R, Wang Y-L, Zhao H, Ye C-Z, Liang G-H and Zong H-S 2021 *Results Phys* **22** 103974
[10] Ehrenfest P 1909 *Physikalische Zeitschrift* **10** 918
[11] Rizzi G and Ruggiero M L 2003 *Relativity in Rotating Frames: Relativistic Physics in Rotating Reference Frames* vol 135 (Dordrecht: Kluwer)
[12] Atanasov V and Dandoloff R 2015 *Phys. Scr.* **90** 065001
[13] Yannoni C S, Johnson R D, Meijer G, Bethune D S and Salem J R 1991 *J. Phys. Chem.* **95** 9
[14] Strzhemechny M A and Katz E A 2005 *Fuller Nanotub Car* N **12** 281
[15] Zou Y *et al* 2009 *Proc Natl Acad Sci USA* **106** 22135
[16] Fakrach B, Fergani F, Boutahir M, Rahmani A, Chadli H, Hermet P and Rahmani A 2018 Structure and raman spectra of c60 and c70 fullerenes encased into single-walled boron nitride nanotubes: a theoretical study *Crystals* **8** 118
[17] Takahata K 2013 *Advances in Micro/nano Electromechanical Systems and Fabrication Technologies* (BoD-Books on Demand)
[18] Prinz V Y, Seleznev V A, Gutakovsky A K, Chehovskiy A V, Preobrazhenskii V V, Putyato M A and Gavrilova T A 2000 *Phys.* E **6** 828
[19] Ozaki T, Iwasa Y and Mitani T 2000 *Phys. Rev. Lett.* **84** 1712
[20] Schmidt O G and Eberl K 2001 *Nature* **410** 168
[21] Fennimore A M, Yuzvinsky T D, Han W-Q, Fuhrer M S, Cumings J and Zettl A 2003 *Nature* **424** 408
[22] Král P and Sadeghpour H R 2002 *Phys. Rev.* B **65** 161401
[23] Sadeghpour H R and Granger B E 2004 *Phys. Scr.* T **T110** 262
[24] Fan D L, Zhu F Q, Cammarata R C and Chien C L 2005 *Phys. Rev. Lett.* **94** 247208
[25] Lima J R F, Brandão J, Cunha M M and Moraes F 2014 *Eur. Phys. J.* D **68** 94
[26] Lima J R F and Moraes F 2015 *Eur. Phys. J.* B **88** 63
[27] Cunha M M, Brandão J, Lima J R F and Moraes F 2015 *Eur. Phys. J.* B **88** 288
[28] Lima J R F, de Pádua Santos A, Cunha M M and Moraes F 2018 *Phys. Lett.* A **382** 2499
[29] Jensen H and Koppe H 1971 *Ann. Phys.* **63** 586
[30] da Costa R C T 1981 *Phys. Rev.* A **23** 1982
[31] Wang Y-L and Zong H-S 2016 *Ann. Phys.* **364** 68
[32] Ferrari G and Cuoghi G 2008 *Phys. Rev. Lett.* **100** 230403
[33] Wang Y-L, Du L, Xu C-T, Liu X-J and Zong H-S 2014 *Phys. Rev.* A **90** 042117
[34] Schuster P and Jaffe R 2003 *Ann. Phys.* **307** 132